ILASS Americas 26th Annual Conference on Liquid Atomization and Spray Systems, Portland OR, May 2014

Modification of the CAB Model for Air-Assist Atomization of Food Sprays

F. X. Tanner[1*], K. A. Feigl[1], O. Kaario[2], B. Dubey[3] and E. J. Windhab[3]

[1]Department of Mathematical Sciences, Michigan Technological University, Houghton, MI 49931, U.S.A.
[2]Aalto University School of Engineering, FIN-00076, Aalto, Finland
[3]Institute of Food, Nutrition and Health, ETH Zurich, CH-8092 Zurich, Switzerland

Abstract

The Cascade Atomization and Drop Breakup (CAB) model has been originally developed for pressure atomizers. In this study, the CAB model is modified to accommodate the atomization of low-pressure, air-assist atomizers. The modifications include the first breakup which is modeled by estimating the Weber number due to the increased liquid-gas relative velocity caused by the air flow. This breakup depends on whether the Weber number is in the catastrophic, stripping or bag breakup regime. The second modification includes a change in the product drop distributions, namely, instead of a uniform distribution, as used in the original CAB model, a χ-squared distribution with the same average drop size is assumed. The model changes are validated with experimental data obtained by means of two different air-assist atomizers using an oil-in-water emulsion. The simulations are performed with a modified version of the *KIVA-3* CFD code; they show good agreement with the experiments.

*Corresponding author: tanner@mtu.edu

INTRODUCTION

Powders play an important role in food processing. They can be a final product or merely represent an intermediate step in a more complex process. Powdered substances can be obtained by means of spray-drying or spray-freezing. Depending on the application, this powder is required to have specific macroscopic properties such as a desired particle size distribution, and microscopic structures which contain exact amounts of certain components (e.g. nutrients) in each particle. Therefore, the liquids involved in food sprays can be very complex, typically consisting of multi-phase/multi-component suspensions or emulsions, which have anisotropic structure and can exhibit non-Newtonian and even viscoelastic behavior. Consequently, high-pressure atomizers are not suited for food sprays because the high pressures needed in this process could alter the complex material structures and thus change essential material characteristics such as taste and shelf life.

Utilizing pressure atomizers at low injection pressures is also not an option, as a computational investigation of a highly viscous liquid spray revealed (cf. Ref. [1]). In fact, it was shown that an injection pressure doubling from 6 bar to 12 bar had almost no influence on the average drop size. The reason for this behavior was the fact that the average drop Weber numbers[1] were mainly subcritical, i.e., less than $We_{crit} = 12$, and therefore, there was only insignificant breakup activity. In addition, the average drop sizes were considerably larger than required. Smaller nozzle orifices (which would result in smaller droplets) were not an option as they were prone to clogging of the nozzle.

These investigations support the fact that in food-related sprays air-assist atomizers are widely used. In air-assist atomizers, the liquid exiting the nozzle interacts with air jets which leads to the liquid breakup. The interaction between the air and the liquid jets is a complex multi-scale problem which cannot be resolved for a realistic spray by present-day computers. Therefore, the simulation of an air-assist atomizer poses a modeling challenge which is the subject of the present study; it constitutes a further development of the air-assist atomization model introduced in Ref. [1].

The modeling approach taken in this study is based on the Cascade Atomization and Drop Breakup (CAB) model of Tanner [2]. The CAB model describes the atomization of a high-speed liquid jet, also referred to as the *primary breakup*, and it also describes the *secondary breakup* of droplets farther downstream. The primary breakup is modeled by injecting large droplets of orifice size which subsequently break up into tiny droplets via a cascade of drop decays, until the droplets reach a stable state. Each individual breakup event is caused by aerodynamic instabilities and its nature depends on the drop Weber number. More precisely, the breakups are modeled after the experimentally observed bag, stripping, and catastrophic breakup regimes.

In an air-assist nozzle, the interaction of the air stream with the liquid jet increases the relative velocity between the gas and the liquid. This increases the Weber number and hence determines the liquid breakup. This liquid-gas interaction depends on the nozzle design and occurs only within a short distance near the liquid nozzle exit. Therefore, the air-assisted breakup occurs exactly once, and it is modeled using the breakup criteria of the CAB model, taking the increased Weber number into account. After the initial breakup, the droplets are subject to the usual air-droplet interaction described by the standard CAB model.

In addition to the first breakup modeling, the uniform product droplet assumption used in the standard CAB model results in unrealistic product drop size distributions. Therefore, the product droplets are equipped with a χ-squared distribution which has the same mean value as the uniform distribution used in the original CAB model.

The air-assist breakup model has been validated with experimental drop size distributions obtained from sprays of an oil-in-water emulsion for two different type of air-assist atomizers. The corresponding simulations have been performed with a modified version of a Kiva-3-based CFD code.

BREAKUP MODELING

First, a summary of the standard CAB model for high-pressure sprays is given, followed by a detailed description of the primary breakup for the air-assist atomization process.

The CAB Drop Breakup Model

The basic idea of the CAB model is the simulation of individual breakup events which are modeled after the experimentally observed bag, stripping or

[1] The Weber number is defined as $We = \rho_g d v_r^2/\sigma$, where ρ_g is the gas density, d the drop diameter, v_r the relative gas-drop velocity, and σ is the surface tension.

catastrophic breakup mechanism, as reported by Liu and Reitz [3]. The actual breakup criterion of a single drop is determined from the Taylor drop oscillator [4] as introduced by O'Rourke and Amsden [5] in the context of spray simulations. In this approach, the drop distortion is described by a forced, damped, harmonic oscillator where the forcing term is given by the aerodynamic droplet-gas interaction, the damping is due to the liquid viscosity and the restoring force is supplied by the surface tension. Breakup occurs when the normalized drop distortion exceeds the critical value of one.

The behavior of the product droplets is derived from a drop creation rate equation, which, in conjunction with mass conservation and a uniform product drop size distribution assumption, leads to the relation

$$\frac{r}{a} = e^{-K_{bu} t_{bu}}, \tag{1}$$

where a and r are the radii of the parent and product drops, respectively, t_{bu} is the breakup time, and K_{bu} is the breakup frequency which depends on the breakup regime. These breakup regimes are classified with respect to increasing gas Weber numbers into bag breakup ($We_{crit} < We \leq We_{b,s}$), stripping breakup ($We_{b,s} < We \leq We_{s,c}$) and catastrophic breakup ($We > We_{s,c}$), where the regime-dividing Weber numbers are taken to be $We_{crit} = 12$, $We_{b,s} = 80$ and $We_{s,c} = 350$, as suggested in Liu and Reitz [3].

More formally, the breakup frequency can be expressed as

$$K_{bu} = \begin{cases} k_1\omega & \text{if} \quad We_{crit} < We \leq We_{b,s} \\ k_2\omega\sqrt{We} & \text{if} \quad We_{b,s} < We \leq We_{s,c} \\ k_3\omega We^{3/4} & \text{if} \quad We_{s,c} < We \end{cases} \tag{2}$$

wherethe drop oscillation frequency, ω, is given by

$$\omega^2 = \frac{8\sigma}{\rho_l a^3} - \frac{25\mu_l^2}{4\rho_l^2 a^4}.$$

In this equation, σ denotes the surface tension, ρ_l the liquid density, a the drop radius and μ_l the liquid viscosity.

The breakup frequency, K_{bu}, in the bag breakup and the stripping breakup regime is proportional to the characteristic breakup frequencies suggested by O'Rourke and Amsden [5]. The characteristic breakup frequency for the catastrophic breakup regime is derived from the study of the Rayleigh-Taylor instability by Bellman and Pennington [6], as reported by Patterson and Reitz [7]. The constant $k_1 = 0.05$ has been determined such that the drop radii match the phase Doppler measurements of Schneider [8], whereas the values for the constants k_2 and k_3 are chosen such that K_{bu} is continuous at the regime-dividing Weber numbers, $We_{b,s}$ and $We_{s,c}$.

An additional property of the product droplets are their initial velocities. The axial velocity is inherited from the parent drop, whereas the transversal (radial) velocity, which contributes to the radial expansion of the spray, is derived from an energy conservation argument involving the surface, kinetic and deformation energies of the parent and product drops (cf. Ref. [2]).

High-Pressure Atomization Modeling

The original CAB model presented in Ref. [2] has been developed for pressure atomizers. The atomization of a high-speed liquid jet results in a *fragmented* liquid core at the nozzle exit (cf. Refs. [9] and [10]). This fragmented liquid core is simulated by injecting large drops of the size of the nozzle orifice. These drops eventually break up into smaller product droplets until they reach a stable state, thus forming a breakup cascade where each breakup event is governed by the cascade breakup law given in Eq. (1). The initial breakup time of these large drops, t_{bu}, is obtained from the experimental jet breakup length correlation due to Levich [11]

$$L = v_{inj} t_{bu} = C_\lambda \sqrt{\frac{\rho_l}{\rho_g}} d_0, \tag{3}$$

where d_0 is the nozzle diameter and v_{inj} the jet exit velocity. The constant C_λ is nozzle dependent, and for the pressure atomizer considered in the original model tuning described in Ref. [2], a value of C_λ=5.5 has been used.

In order to account for the droplet surface stripping near the nozzle exit, the initially injected drops have been equipped with an initial drop size distribution (IDSD) such that the small droplets reflect the surface stripping and the large drops yield good penetration and simulate the fragmented liquid core. For high-pressure sprays, this (integral) drop size distribution is formally given by the power law

$$H(d) = \begin{cases} \left(\frac{d}{d_o}\right)^{n+1} & \text{if} \quad 0 < d < d_0 \\ 0 & \text{otherwise} \end{cases} \tag{4}$$

where d and d_o are the drop and nozzle radii, respectively. The model tuning described in Ref. [2] has resulted in a value of $n = 0.5$.

C_λ	jet breakup length coefficient	5.5
θ	spray angle	Eq. (5)
k_1	breakup regime constant	0.05
n	IDSD: power law exponent	0.5

Table 1. Constants used in the CAB model for high-pressure sprays.

In the CAB model, the spray angle, θ, is prescribed as an initial condition. For pressure atomizers, the values are the ones from the experimental correlation of Naber and Siebers [12] given by

$$\tan(\theta/2) = 0.31\left(\frac{\rho_g}{\rho_d}\right)^{0.19}. \qquad (5)$$

The CAB model constants for high-speed liquid jets are summarized in Table 1. The constants θ and C_λ depend on the nozzle and on the injection system specific properties and, in general, need to be adjusted in order to compensate for such influences.

Air-Assist Atomization Modeling

Modeling of the product droplet distribution. In the original CAB model, the product droplet distribution is taken to be uniform, i.e., after a breakup all product droplets have the same diameter determined by Eq. (1). The uniform product drop size assumption works well for high-pressure sprays because the initially injected large drops fall into the catastrophic breakup regime and therefore, they undergo several breakups (in different breakup regimes) until they reach a stable state. Also, it should be noted that the uniform product drop size assumption is realistic for the stripping breakup regime.

For low-pressure sprays, however, the initially injected droplets are either stable or they fall into the bag breakup regime, which means that the product droplets are not uniform. Consequently, the assumption of a uniform product drop size distribution is unrealistic. This is also the case for air-assist atomizers, because the air jet causes the first drop breakup at high Weber numbers (usually in the catastrophic regime), whose product droplets are in general not uniform.

To describe a more realistic non-uniform product drop behavior, the product droplets are assumed to follow a χ-squared distribution whose mean value corresponds to the product droplet radius determined via Eq. (1). More precisely, the χ-squared droplet distribution is given by

$$f(r) = \frac{1}{\bar{r}}\exp(-r/\bar{r}),$$

where $\bar{r}$ is the mean drop size determined by Eq. (1). Observe that $\bar{r} = \int_0^\infty r f(r) dr$, i.e., $\bar{r}$ is also the mean value of the χ-squared distribution. Consequently, Eq. (1) is to be interpreted as determining the mean values of the product droplet distributions.

C_λ	jet breakup length coefficient	0.5
θ	spray angle	Eq. (5)
k_1	bag breakup constant	1
k_2	stripping breakup constant	13
k_3	catastrophic breakup constant	30
$\bar{r}_o$	IDSD: χ^2-distribution	$254\mu m$

Table 2. Constants used in the CAB model for air-assist atomizers.

Also, for low-pressure sprays there is no surface stripping at the nozzle exit and the IDSD power law in Eq. (4) is not relevant. As an alternative, the IDSD was taken to follow a χ-squared distribution whose mean value $\bar{r}_o$ corresponds to the nozzle orifice radius.

In the actual program implementation, the drop distributions are discretized into parcels, where each parcel is a collection of droplets of equivalent states (cf.Ref. [13]). In particular, each parcel contains drops of identical mass, and therefore, the χ-squared distribution for the drop radii becomes the volume-weighted density distribution for the parcels

$$g(r) = \frac{1}{A} r^3 f(r).$$

The normalization $\int_0^\infty g(r)dr = 1$ yields $A = 6\bar{r}^3$ and, therefore, the χ-squared parcel distribution becomes

$$g(r) = \frac{1}{6}\left(\frac{r}{\bar{r}}\right)^3 \frac{1}{\bar{r}}\exp(-r/\bar{r}). \qquad (6)$$

Eq. (6) is the actual distribution used in the modeling of the product drop sizes. The difference between the χ-squared distribution and the volume-weighted χ-squared distribution is illustrated in Fig. 1 for a hypothetical case with $\bar{r} = 100\ \mu m$.

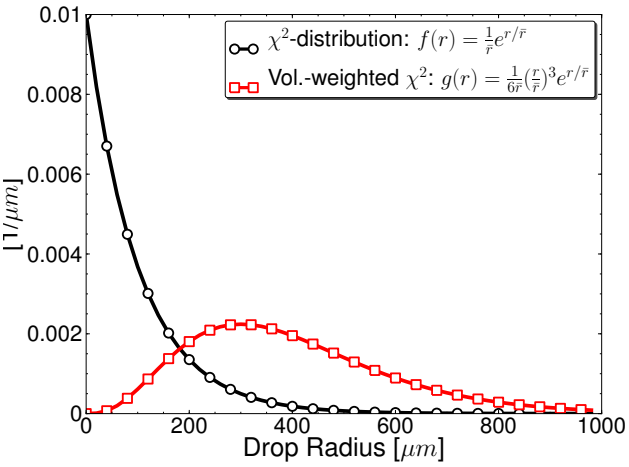

Figure 1. χ-squared and volume-weighted χ-squared distributions for a hypothetical case with $\bar{r} = 100\ \mu m$.

Modeling of the interaction between the liquid and the gas jets. In an air-assist atomizer, the air jet increases the relative gas-liquid velocity, which increases the gas Weber number, and consequently, aids in the liquid breakup. This air-liquid interaction occurs only in a small region of the liquid jet at the nozzle exit and, therefore, influences only the first breakup.

Two different type of air-assist atomizers have been used in this study: an internal mixing type (referred to as inmix and labeled as A), and an external mixing type (referred to as exmix and labeled as B). A schematic of the two atomizer types is shown in Fig. 2. In the inmix type, the air jet interacts with the liquid jet inside the nozzle and hence leads to liquid breakup inside the nozzle. In the exmix type atomizer, the interaction between the air jet and the liquid jet occurs just at the nozzle exit. In addition, as can be seen in the nozzle sketch, in the inmix case, the air jet interacts with the liquid jet at an angle, and in the exmix case, the air jet is initially parallel to the liquid jet. The stability of the liquid jet is determined by the gas Weber number, which in turn depends on the norm of the relative liquid-gas velocity

$$||\boldsymbol{u}_r|| = ||\boldsymbol{u}_l - \boldsymbol{u}_g|| = \sqrt{||\boldsymbol{u}_l||^2 + ||\boldsymbol{u}_g||^2 - 2||\boldsymbol{u}_l||||\boldsymbol{u}_g|| \cos\alpha}.$$

In this equation, the second expression reflects the law of cosines, where α is the angle between $\boldsymbol{u}_l$ and $\boldsymbol{u}_g$. Assuming a value of $\alpha = 90^o$ for the inmix nozzle type and $\alpha = 0$ for the exmix nozzle, gives the expressions for the relative velocities of the two nozzle

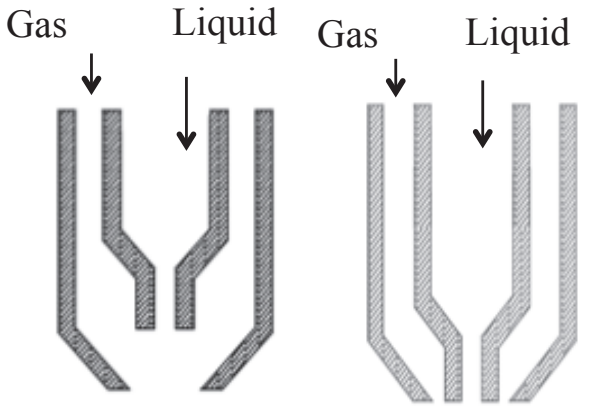

Figure 2. Cross-sections of the inmix nozzle (left) and the exmix nozzle (right).

types as

$$||\boldsymbol{u}_A|| = \sqrt{||\boldsymbol{u}_l||^2 + ||\boldsymbol{u}_g||^2} \quad (7)$$

$$||\boldsymbol{u}_B|| = ||\boldsymbol{u}_l - \boldsymbol{u}_g|| \quad (8)$$

Equations (7) and (8) are the relative velocities used in the calculation of the Weber number for the first breakup in the respective air-assist atomizers.

Adjusting of the model constants. The interaction between the liquid and the gas jets occurs at the nozzle exit. Therefore, the liquid breakup length is considerably shorter than in a corresponding pressure atomizer, and, therefore, the CAB model constant C_λ, which controls the breakup length, was reduced to a value of 0.5. In addition, the breakup regime constants in Eq. (2) were set to $k_1 = 1$, $k_2 = 13$ and $k_3 = 30$. These model constants are summarized in Table 2.

EXPERIMENTAL AND COMPUTATIONAL DETAILS

The spray experiments were conducted at atmospheric pressure and a temperature of 293 K. The injected liquid was a 40% oil-in-water emulsion kept at a temperature of 293 K. At this temperature, the density of the liquid was 977 kg/m^3, the viscosity 0.1799 Pas and the surface tension 0.035 N/m. The latter two were measured by means of a shear rheometer and the pendant-drop method, respectively. The material properties and spraying conditions are summarized in Table 3. Experiments were performed for the inmix and exmix air-assist nozzles

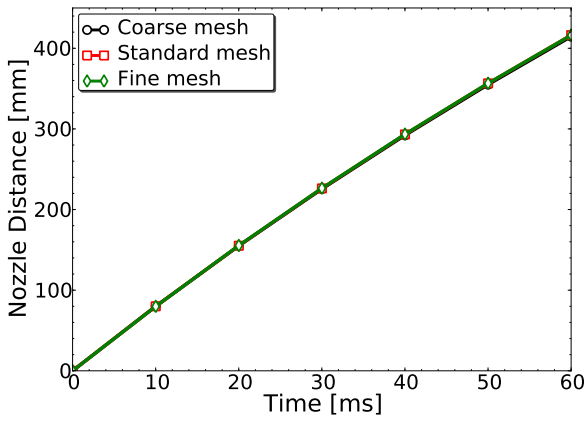

Figure 3. Mesh dependence of the spray penetration for the inmix nozzle case A3.

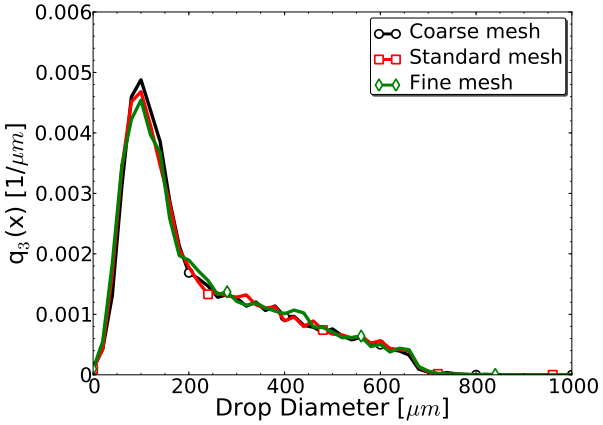

Figure 4. Mesh dependence of the volume-weighted drop size distribution at 20 cm downstream from the nozzle exit for the inmix nozzle case A3.

sketched in Fig. 2 at different nozzle air flows but constant liquid flow rates. The spray droplets were measured at 20 cm downstream from the nozzle exit. The drop size distributions were obtained by means of a *Spraytec* laser diffraction device (Malvern Instruments, Lens: 750 mm).

The computations presented in this study were performed with a modified version of the *KIVA-3* code [13] equipped with various new or improved models. As described above, a revised version of the CAB atomization and drop breakup model was utilized to model the air-assist atomization. The turbulence was accounted for via the *RNG k-ε* turbulence model as implemented by Han and Reitz [14]. Unless stated otherwise, all the standard values of the model parameters, as reported in the respective citations, were used.

Parameter	**Value**
Ambient gas	air
Ambient temperature	293 K
Ambient pressure	1 bar
Liquid nozzle diameter	0.5 mm
Liquid temperature	293 K
Liquid density	977 kg/m^3
Liquid viscosity	0.1799 Pas
Liquid surface tension	0.035 N/m
Liquid Injection flow rate	100 ml/min
Liquid Injection velocity	8.49 m/s

Table 3. Process conditions in the air-assist model validations.

The computational domain was a closed cylinder of diameter 30 cm and length 55 cm. The injector head was depicted as a co-axial cylinder of diameter 4.3 cm and length 5 cm, protruding into the computational domain at the top of the cylinder. The computational meshes utilized are structured, hexahedral, polar meshes whose cells are concentrated radially and vertically around the injector, that is, around the nozzle exit. The cylinder part of the standard mesh has $35 \times 20 \times 75$ (52'500) cells in radial, azimuthal and axial directions. The smallest cell is at the nozzle exit measuring approximately 1.5 mm by 1.5 mm in radial and axial direction.

Mesh Dependence Study

The mesh dependence of the air-assist model has been investigated in terms of the spray penetration and the volume-weighted drop size distribution at 20 cm downstream from the nozzle exit for the inmix nozzle case A3 (cf. Table 4). The coarse and the fine mesh were obtained from the standard mesh by reducing, respectively, increasing, the number of cells in each direction by a factor of 1.5. This lead to the coarse mesh with $24 \times 13 \times 50$ (15'600) cells, and the fine mesh with $52 \times 30 \times 112$ (174'720) cells in radial, azimuthal, and axial directions.

The results of this mesh refinement study are shown in Figs. 3 and 4. Figure 3 shows that the penetrations are virtually mesh independent, and Fig. 4 illustrates the mesh independence for the drop size distributions. These results justify the choice of the standard mesh for all subsequent computations.

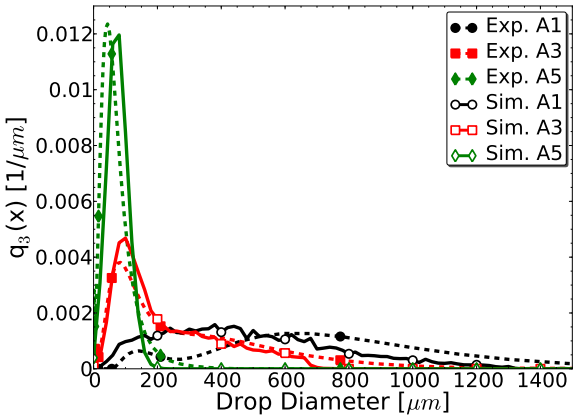

Figure 5. Volume-weighted drop size distributions at 20 cm downstream for the inmix nozzle cases A1, A3 and A5. The filled symbols denote the experiments and the open symbols the simulations.

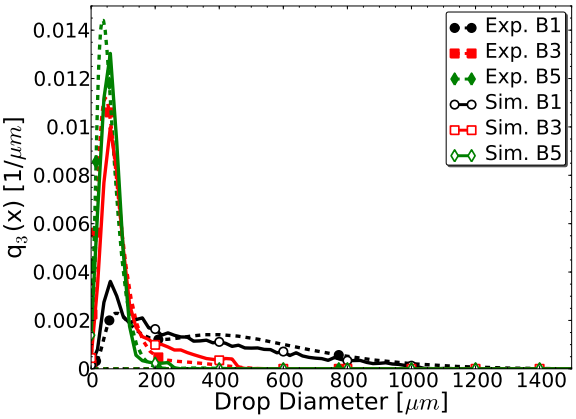

Figure 6. Volume-weighted drop size distributions at 20 cm downstream for the exmix nozzle cases B1, B3 and B5. The filled symbols denote the experiments and the open symbols the simulations.

AIR-ASSIST MODEL VALIDATIONS

The modifications of the CAB model were validated with experimental drop size distributions for various air-flows of the inmix (type A) and the exmix (type B) air-assist nozzles. As discussed previously, the CAB model constants used in the simulations were the values listed in Table 2.

The air-flow conditions are summarized in Table 4 together with the average gas Weber numbers of the initial drop size distributions. Recall that the relative velocities used in the calculation of the Weber numbers are obtained by means of Eqs. (7) and (8). Keeping in mind that the transition Weber numbers are $We_{b,s} = 80$ and $We_{s,c} = 350$, it follows that the initial breakup of the inmix Case A1 falls into the bag breakup regime, the inmix Case A3 is a stripping breakup and the Case A5 is a catastrophic breakup. The initial Weber numbers of the exmix cases are higher and only Case B1 falls into the stripping breakup regime, whereas Cases B3 and B5 fall into the catastrophic regime.

Case	Air flow	Air exit velocity	We_g
Inmix A1	25 l/min	56.68 m/s	58
Inmix A3	35 l/min	79.35 m/s	111
Inmix A5	77 l/min	174.76 m/s	533
Exmix B1	10 l/min	137.05 m/s	288
Exmix B3	15 l/min	205.57 m/s	677
Exmix B5	20 l/min	274.10 m/s	1229

Table 4. Simulation cases: variations of the nozzle air flow and the associated average gas Weber numbers.

For the inmix nozzle type, the results of these comparisons are shown in Fig. 5 in terms of the volume-weighted drop size distributions at 20 cm downstream from the nozzle exit. As expected, the larger air-flows produce distributions with smaller droplets, that is, the distribution peaks are shifted to the left. This is a direct consequence of the fact that the higher Weber number breakups produce smaller droplets. As can be seen from this figure, the agreement between the simulations and the experiments is good for the two larger air-flows. For the smallest air-flow (Case A1) the experimental drop size distribution exhibits a double peak which is not reproduced by the simulation. However, as can be seen from the figure, the average drop sizes of the experiments and the simulations are close in all cases.

The results of the external-mixing-nozzles are compared in Fig. 6. Again, as in the inmix cases, the larger air-flows result in drop size distributions with smaller droplets, but the shift of the distribution peaks is not as pronounced as for the inmix cases. This can be explained by the fact that the initial breakups of both Cases B3 and B5 are catastrophic, which results in almost identical drop size distributions. The fact that the initial drop breakups in Case B1 fall into the stripping breakup regime re-

sults in a drop size distribution with larger droplets. Again, as for the inmix cases, the agreement between the experimental and simulated drop size distributions can be considered as good.

SUMMARY AND CONCLUSIONS

The CAB model has been modified to accommodate atomization processes for an inmix and an exmix air-assist atomizer. The modifications include a change in the product drop distributions. Instead of a uniform distribution, as used in the original CAB model, a χ-squared distribution with the same average drop size has been utilized. In the actual implementation, a volume-weighted distribution has been used in order to account for the parcel discretization of the spray probability distribution function.

The second modification addresses the air-assist atomization process. This process has been modeled by estimating the Weber number due to the increased relative velocity caused by the air jet. The relative velocities were computed differently, depending on whether the nozzle is inmix or exmix. The interaction between the liquid and the air jets leads to exactly one breakup whose characteristics depends on whether the Weber number is in the catastrophic, stripping or bag breakup regime.

The model changes have been validated with experimental data obtained from an oil-in-water emulsion. The simulations were performed with a *KIVA-3*-based code which is equipped with well-established spray models. Overall, the validations showed good agreement with the experimental data.

References

[1] F. X. Tanner, K. A. Feigl, T. O. Althaus, and E. J. Windhab, Modeling and Simulation of an Air-Assist Atomizer for Food Sprays, *Proc. 21st ILASS-Americas Annual Conference*, Orlando, FL, May 2008. CD ROM Publication.

[2] F. X. Tanner, Development and Validation of a Cascade Atomization and Drop Breakup Model for High-Velocity Dense Sprays, *Atomization and Sprays*, vol. 14, no. 3, pp. 211–242, 2004.

[3] A. B. Liu and R. D. Reitz, Mechanisms of Air-Assisted Liquid Atomization, *Atomization and Sprays*, vol. 3, pp. 55–75, 1993.

[4] G. I. Taylor, The Shape and Acceleration of a Drop in a High Speed Air Stream, *The Scientific Papers of Sir Geoffrey Ingram Taylor* (G. K. Batchelor, ed.), vol. 3, pp. 457–464, Cambridge University Press, 1963.

[5] P. J. O'Rourke and A. A. Amsden, The TAB Method for Numerical Calculation of Spray Droplet Breakup, SAE Paper 872089, 1987.

[6] R. Bellman and R. H. Pennington, Effects of Surface Tension and Viscosity on Taylor Instability, *Quarterly of Applied Mathematics*, vol. 12, no. 2, 1954.

[7] M. Patterson and R. D. Reitz, Modeling the Effects of Fuel Spray Characteristics on Diesel Engine Combustion and Emission, SAE Paper 980131, 1998.

[8] B. Schneider, Experimental Investigation of Diesel Sprays, CRFD and Laser Diagnostic Workshop, 21st CIMAC Congress 1995, Interlaken, Switzerland, May 1995.

[9] O. L. Gülder, Temporally and Spatially Resolved Drop Sizing of Dense Diesel Sprays, ASME Paper 87-FE-5, 1987.

[10] F. X. Tanner, K. A. Feigl, S. A. Ciatti, C. F. Powell, S.-K. Cheong, J. Liu, and J. Wang, Structure of High-Velocity Dense Sprays in the Near-Nozzle Region, *Atomization and Sprays*, vol. 16, pp. 579–597, 2006.

[11] V. G. Levich, *Physicochemical Hydrodynamics*, Prentice–Hall, Englewood Cliffs, N.J., pp. 639–650, 1962.

[12] J. Naber and D. Siebers, Effects of Gas Density and Vaporization on Penetration and Dispersion of Diesel Sprays, *SAE Transactions: Journal of Engines*, vol. 105, no. 3, 1997.

[13] A. A. Amsden, P. J. O'Rourke, and T. D. Butler, KIVA II: A Computer Program for Chemically Reactive Flows with Sprays, Tech. Rep. LA-11560-MS, Los Alamos National Laboratory, May 1989.

[14] Z. Y. Han and R. D. Reitz, Turbulence Modeling of Internal Combustion Engines Using *RNG* k-ε Models, *Combustion Science and Technology*, vol. 106, pp. 267–295, 1995.